eng

MDPI

Article

Comprehensive Investigation into the Thermal Performance of Nanofluid-Enhanced Heat Pipes for Advanced Thermal Management Systems

Mohan Govindasamy [1], Manikandan Ezhumalai [1], Ratchagaraja Dhairiyasamy [2,*], Deekshant Varshney [3,4], Subhav Singh [5,6] and Deepika Gabiriel [7]

[1] Department of Mechanical Engineering, University College of Engineering Villupuram, Villupuram 605103, Tamil Nadu, India; mohan@aucev.edu.in (M.G.); manimeice@gmail.com (M.E.)
[2] Department of Electronics and Communication Engineering, Saveetha School of Engineering, Saveetha Institute of Medical and Technical Sciences, Saveetha University, Chennai 602105, Tamilnadu, India
[3] Centre of Research Impact and Outcome, Chitkara University, Rajpura 140417, Punjab, India; profvarshney@outlook.com
[4] Division of Research & Innovation, Uttaranchal University, Dehradun 248007, Uttarakhand, India
[5] Chitkara Centre for Research and Development, Chitkara University, Baddi 174103, Himachal Pradesh, India; er.subhav@hotmail.com
[6] Division of Research and Development, Lovely Professional University, Phagwara 144411, Punjab, India
[7] College of Engineering and Technology, Aksum University, Tigray, Aksum 1010, Ethiopia; gabirieldee@gmail.com
* Correspondence: ratchagaraja@gmail.com

Abstract: This study investigates the thermal performance of heat pipes using nanofluids based on silver (Ag), aluminum oxide (Al_2O_3), and multi-walled carbon nanotubes (MWCNTs) at varying concentrations. Heat pipes, recognized for their efficiency in passive thermal management, face limitations with traditional fluids. Nanofluids, engineered by dispersing nanoparticles in base fluids, were explored as alternatives due to their superior thermal conductivity and convective properties. Nanofluids were prepared using ultrasonication, and their thermal conductivity, viscosity, and stability were evaluated. Experimental tests were conducted under controlled conditions to assess the impact of nanoparticle type, concentration, inclination angle, and fluid filling ratio on performance metrics, including thermal resistance (TR) and heat transfer coefficients (HTCs). The results demonstrated that Ag-based nanofluids outperformed others, achieving a 150% increase in thermal conductivity and an 83% reduction in TR compared to deionized water. HTCs increased by 300% for Ag nanofluids at a 0.5% concentration. Inclination angles and filling ratios also significantly affected performance, with optimal conditions identified at a 70% filling ratio and a 30° inclination angle. The findings highlight the potential of nanofluids in optimizing heat transfer systems and provide a framework for selecting suitable parameters in industrial applications.

Keywords: nanofluids; heat pipes; thermal conductivity; heat transfer coefficient; aluminum oxide

check for updates

Academic Editor: Dimitris S. Achilias

Received: 3 January 2025
Revised: 8 March 2025
Accepted: 14 March 2025
Published: 17 March 2025

Citation: Govindasamy, M.; Ezhumalai, M.; Dhairiyasamy, R.; Varshney, D.; Singh, S.; Gabiriel, D. Comprehensive Investigation into the Thermal Performance of Nanofluid-Enhanced Heat Pipes for Advanced Thermal Management Systems. *Eng* **2025**, *6*, 55. https://doi.org/10.3390/eng6030055

Copyright: © 2025 by the authors. Licensee MDPI, Basel, Switzerland. This article is an open access article distributed under the terms and conditions of the Creative Commons Attribution (CC BY) license (https://creativecommons.org/licenses/by/4.0/).

1. Introduction

The increasing demand for efficient thermal management systems in various industries, including electronics cooling, renewable energy, and aerospace, has intensified research efforts into advanced heat transfer technologies. Heat pipes, as passive heat transfer devices, have gained significant attention due to their ability to transfer large

quantities of heat with minimal temperature gradients. However, the performance of conventional heat pipes is largely dictated by the thermal properties of the working fluid, which imposes limitations on their efficiency [1]. To overcome these constraints, the use of nanofluids—engineered suspensions of nanoparticles in a base fluid—has emerged as a promising solution. Heat pipe performance is primarily evaluated based on TR and HTCs. A well-performing heat pipe demonstrates minimal TR, high HTCs, and a uniform temperature gradient. These factors are influenced by the properties of the working fluid, filling ratio, inclination angle, and operating conditions. The present study systematically investigates these parameters to establish an optimized working range for enhanced heat transfer. Nanofluids are known to exhibit enhanced thermal conductivity, specific heat capacity, and convective heat transfer properties compared to traditional fluids such as water or ethylene glycol. These unique characteristics position nanofluids as potential game-changers in the field of heat transfer.

Despite the substantial progress made in the development of nanofluids, several challenges persist. One critical issue is the selection of nanoparticle types and concentrations that maximize thermal performance without compromising stability and flow characteristics. Commonly used nanoparticles include metals such as silver (Ag), metal oxides like aluminum oxide (Al_2O_3), and carbon-based materials such as multi-walled carbon nanotubes (MWCNTs). Each nanoparticle type offers distinct advantages; for example, silver nanoparticles exhibit extremely high thermal conductivity, while MWCNTs provide unique structural properties that enhance capillary action in heat pipes [2]. However, the relative performance of these nanofluids under identical operating conditions remains poorly understood. Additionally, factors such as nanoparticle concentration, inclination angle of the heat pipe, and fluid filling ratio have not been comprehensively analyzed to establish optimal working conditions [3].

The growing interest in nanofluids has led to numerous experimental and theoretical studies. For instance, researchers demonstrated the potential of nanofluids to enhance thermal conductivity, sparking widespread interest in this field [4]. Subsequent studies have explored the use of metallic and oxide nanoparticles to improve the thermal properties of working fluids. For example, researchers reported that the thermal conductivity of water-based Al_2O_3 nanofluids increased by up to 30% at low concentrations. Similarly, a study by another researcher demonstrated significant enhancements in convective HTCs using MWCNT nanofluids [5]. However, despite these advancements, discrepancies in experimental results and the lack of standardization in nanofluid preparation methods have hindered the widespread adoption of these technologies [6].

Recent advancements in nanotechnology have opened new avenues for tailoring the properties of nanofluids to specific applications. For example, the use of surfactants and advanced dispersion techniques such as ultrasonication has improved the stability of nanofluids, addressing one of the primary challenges associated with sedimentation and aggregation. However, the interplay between thermal performance and stability remains an area requiring further investigation. Furthermore, while most studies have focused on individual nanofluids, comparative analyses of multiple nanoparticle types under identical conditions are scarce. This gap in the literature highlights the need for systematic studies that evaluate the performance of nanofluids across a range of parameters, including nanoparticle concentration, heat input, and operating temperature [7].

The significance of this research lies in its potential to advance the understanding and application of nanofluids in thermal management systems. By systematically comparing the performance of Ag, Al_2O_3, and MWCNT nanofluids in heat pipes, this study aims to provide valuable insights into their relative advantages and limitations. The use of nanofluids not only enhances the thermal performance of heat pipes but also extends

their applicability to high-heat-flux environments where traditional working fluids fail to meet efficiency requirements. Moreover, the findings of this study could contribute to the development of standardized guidelines for nanofluid preparation and testing, thereby facilitating their adoption in industrial applications [8].

Unlike previous studies that primarily focus on single nanofluids or isolated parameters, this research adopts a holistic methodology that encompasses multiple nanoparticle types, varying concentrations, and critical operating conditions. The inclusion of a detailed uncertainty analysis further distinguishes this work, ensuring the reliability and reproducibility of the results. Additionally, the study incorporates advanced characterization techniques such as UV–visible spectrophotometry for stability analysis and differential scanning calorimetry for specific heat capacity measurements, providing a robust framework for evaluating nanofluid properties [9].

The primary objective of this research is to investigate the thermal performance of heat pipes using Ag, Al_2O_3, and MWCNT nanofluids. Specific objectives include determining the impact of nanoparticle type and concentration on thermal conductivity, viscosity, specific heat capacity, and stability; evaluating the effects of operating conditions such as heat input, fluid filling ratio, and inclination angle; and conducting a comparative analysis with deionized water to quantify performance enhancements. Additionally, the study aims to identify optimal working conditions for each nanofluid to maximize heat transfer efficiency while minimizing flow resistance and stability issues [10].

This research addresses critical gaps in the current understanding of nanofluids in heat pipe applications. By systematically analyzing the performance of multiple nanoparticle types under identical conditions, this study aims to provide a comprehensive framework for optimizing nanofluid-based thermal management systems. The findings are expected to advance the development of high-performance heat pipes and contribute to the broader adoption of nanofluids in industrial applications.

2. Materials and Methods

This study investigates the thermal performance of heat pipes using nanofluids based on silver (Ag), aluminum oxide (Al_2O_3), and multi-walled carbon nanotubes (MWCNTs) at various concentrations. The study emphasizes thermal conductivity, viscosity, specific heat capacity, density, and stability, along with an uncertainty analysis to quantify experimental errors. The nanofluids were prepared using deionized water (DI water) as the base fluid. Nanoparticles of Ag, Al_2O_3, and MWCNTs were procured from Reinste Nano Ventures Pvt. Ltd. (Noida, India) at a purity of 99.9%. The nanoparticles were initially weighed using an analytical balance from Aczet Pvt. Ltd. (Navi Mumbai, India) with a precision of 0.01 mg. To achieve stable suspensions, nanoparticles were dispersed in DI water with concentrations of 0.1%, 0.2%, 0.3%, and 0.5% by volume. The value was determined through direct experimental measurement using a calibrated KD2 Pro analyzer supplied by AIMIL Ltd. (New Delhi, India). Deionized water was sourced from Merck India Pvt. Ltd. (Mumbai, India) and used as the reference fluid, with three independent measurements conducted to ensure accuracy. The obtained results were validated against manufacturer specifications [11] and the published literature [12–16]. Ultrasonication was applied for one hour at 40 kHz using a sonicator from PCI Analytics Pvt. Ltd. (Mumbai, India) to ensure uniform dispersion. Ultrasonic bath sonication was used for nanoparticle dispersion; however, literature studies indicate that probe sonication provides superior energy transfer and more effective dispersion. The relatively high sedimentation observed in this study suggests that bath sonication alone may not be sufficient for long-term nanofluid stability. A surfactant, cetyltrimethylammonium bromide (CTAB), was obtained from Loba Chemie Pvt. Ltd. (Mumbai, India) and used at 0.1% volume to prevent agglomeration in

MWCNT-based nanofluids. The stability of the nanofluids was verified through sedimentation analysis over 24 h. The specific procedures for preparing the nanofluids are shown in Figure 1. An extended observation period of 48 h was conducted to assess long-term stability. While minor sedimentation was observed beyond 24 h, the dispersion stability of the nanofluids remained sufficient for real-time thermal management applications. The use of surfactants and ultrasonication significantly contributed to prolonged stability by minimizing aggregation and settling.

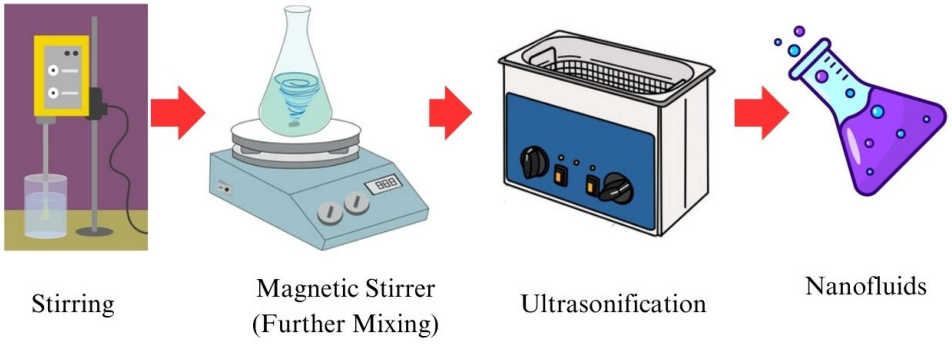


Figure 1. Schematic representation of the nanofluid preparation process.

The SEM images of the nanoparticles used in this study are shown in Figure 2. The SEM images were obtained using a field-emission scanning electron microscope (FESEM, Model: JEOL JSM-7610Fsourced from JEOL India Pvt. Ltd., Mumbai, India) at an accelerating voltage of 10 kV. The images were captured at magnifications ranging from 50,000× to 100,000× to ensure clear visualization of the nanoparticle morphology. The microstructural analysis confirmed the dispersion characteristics and structural integrity of the nanoparticles, which directly impact the thermal performance of the nanofluids. In the Figure 2a, silver (Ag) nanoparticles are observed to exhibit a highly porous and clustered morphology, which is considered advantageous for enhancing thermal conductivity due to the increased surface area. Figure 2b presents aluminum oxide (Al_2O_3) nanoparticles, characterized by plate-like structures with sharp edges and smooth surfaces, which are noted to support capillary-driven flow and heat dissipation in heat pipes. In Figure 2c, the morphology of multi-walled carbon nanotubes (MWCNTs) is illustrated, displaying entangled and fibrous structures forming agglomerates. Figure 2d shows the TEM of the prepared nanofluid [17]. This unique structure is found to contribute to improved thermal performance by facilitating efficient capillary action and thermal conductivity. These distinct morphologies are aligned with the performance trends observed in the experimental analysis, where Ag and MWCNTs are shown to demonstrate superior thermal properties compared to Al_2O_3.

Thermal conductivity was measured using a transient hot-wire method. The uncertainty associated with the KD2 Pro thermal properties analyzer was ±5.2%, aligning with the standard precision of the instrument. This value was obtained by conducting multiple independent measurements and accounting for potential systematic errors in the transient hot-wire method used for thermal conductivity evaluation [18]. A KD2 Pro thermal properties analyzer was employed, and each measurement was repeated three times to minimize random errors. The specific heat capacity of the nanofluids was measured using differential scanning calorimetry (DSC, Model: Netzsch DSC 214 Polyma sourced from Toshvin Analytical Pvt. Ltd., Mumbai, India) at a heating rate of 10 °C/min. Sapphire was used as the reference material for calibration. The measured heat capacity values were found to have an uncertainty of ±3%, ensuring reliable characterization of the thermal energy storage properties [19]. Viscosity was determined using a rotational viscometer with a precision of ±3%, operating at controlled shear rates of 10 s^{-1}. The density of the nanofluids was evaluated using a digital hydrometer at 25 °C. A digital hydrometer (Model: Anton Paar

DMA 35) with a precision of ±0.5% was used for density measurements. The instrument was calibrated before each set of measurements using deionized water as the reference fluid. The associated uncertainty in density readings was estimated to be ±0.3%. Stability analysis was conducted using UV–visible spectrophotometry, where the absorbance of each nanofluid was measured at a 600 nm wavelength over 24 h [11]. Absorption spectroscopy using a UV–visible spectrophotometer (Shimadzu UV-2600, Kyoto, Japan) was conducted to assess the stability of nanofluid dispersions. Absorbance measurements were performed at a wavelength of 600 nm at regular intervals over 48 h. A decrease in absorbance over time indicated nanoparticle sedimentation, with MWCNT-based nanofluids exhibiting the least reduction, followed by Ag and Al_2O_3 nanofluids. The stability of the nanofluids was evaluated by monitoring the relative change in absorbance over time. The results showed that the use of CTAB as a surfactant improved short-term stability; however, longer-term dispersion required enhanced stabilization techniques. The spectrophotometric analysis revealed no significant sedimentation within the experimental duration.

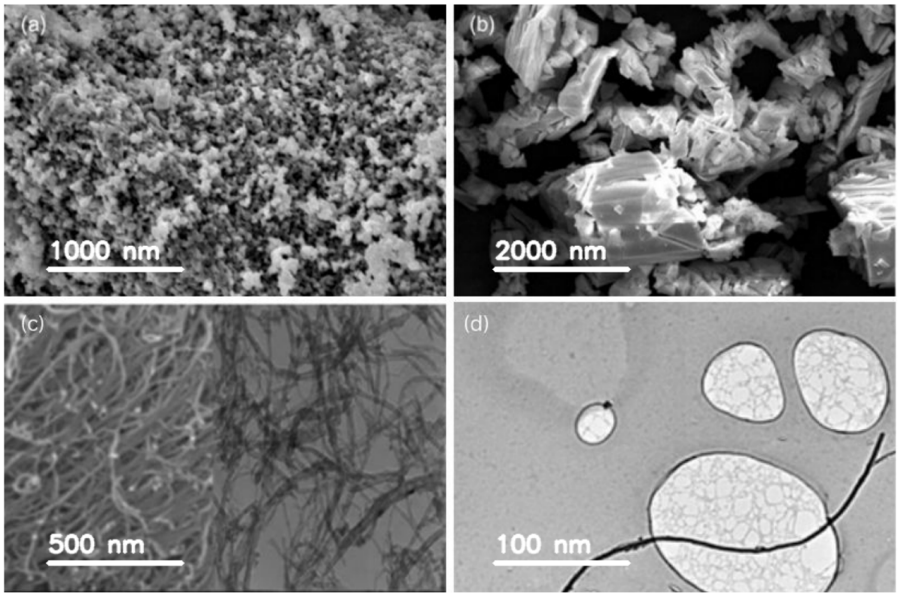


Figure 2. SEM images of (**a**) Ag, (**b**) Al_2O_3, (**c**) MWCNTs, and (**d**) TEM of MWCNT nanofluid.

Figure 3 shows the absorbance decay over time for Ag, Al_2O_3, and MWCNT nanofluids at 600 nm, indicating their relative dispersion stability. Initially, at 0 h, all nanofluids exhibit an absorbance of 1.0, representing a well-dispersed state. Over time, absorbance decreases due to nanoparticle sedimentation, with the rate of decline varying between the nanofluids. At 24 h, Ag nanofluids retain 72% of their initial absorbance, Al_2O_3 nanofluids retain 62%, and MWCNT nanofluids retain 82%. This means that MWCNT-based nanofluids have the slowest decline in absorbance, suggesting better stability. By 48 h, Ag nanofluids exhibit a 50% reduction in absorbance, Al_2O_3 nanofluids drop by 65%, while MWCNT nanofluids only decrease by 32%. The superior stability of MWCNT nanofluids is attributed to the high aspect ratio of carbon nanotubes, which provides stronger interactions with the base fluid, reducing agglomeration. In contrast, Al_2O_3 nanoparticles exhibit the fastest sedimentation rate due to their higher density, causing faster gravitational settling. The presence of a surfactant (CTAB) contributes to the initial dispersion but appears insufficient for long-term stabilization, particularly for Al_2O_3. The improved stability of MWCNTs can be explained by their natural tendency to form stable network-like structures in a fluid medium, which counteracts sedimentation forces. Ag nanofluids, although more stable than Al_2O_3, still experience significant sedimentation, likely due to weaker interparticle repulsion. Figure 4 shows a visual analysis of the prepared nanofluids.

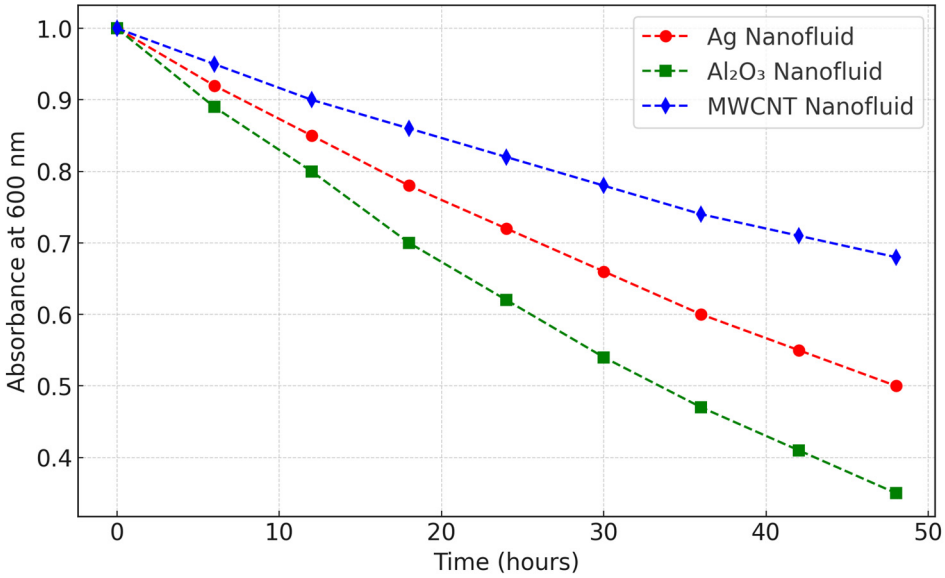


Figure 3. Absorbance decays over time.



Figure 4. Visual stability of mono-nanofluids.

A copper heat pipe with a sintered wick structure was used to evaluate thermal performance. The sintered wick structure within the heat pipe plays a crucial role in capillary-driven flow and heat transfer enhancement (Figure 5). To provide comprehensive insight into its characteristics, the pore diameter, permeability, and porosity were experimentally analyzed. The pore diameter of the sintered wick was determined using scanning electron microscopy (SEM), revealing an average diameter of 20–50 µm. Permeability was assessed based on the Kozeny–Carman equation, yielding a value of 3.8×10^{-12} m^2, which ensures efficient liquid transport. Porosity, a key determinant of liquid retention capability, was measured using the liquid displacement method and found to be 45%, facilitating improved capillary action and thermal performance. These parameters confirm the suitability

of the sintered wick structure in supporting optimal heat pipe function, particularly in nanofluid-based applications. The heat pipe had a length of 200 mm and an outer diameter of 8 mm. The evaporator section was 50 mm long, the adiabatic section was 100 mm, and the condenser section was 50 mm. The heat pipe was filled with nanofluids at filling ratios of 30%, 50%, 70%, and 90% of its internal volume. The filling ratios were determined using a calibrated syringe to ensure precision. The heat input to the evaporator varied from 50 W to 125 W using a controlled DC power supply. A comprehensive evaluation of the thermal performance of heat pipes requires an analysis of the saturation temperature and pressure of the working fluids, as these parameters dictate phase-change efficiency and operational stability. To address this, the saturation temperature (T_{sat}) and saturation pressure (P_{sat}) of the nanofluids were experimentally determined across the operating temperature range of 70 °C to 100 °C using a high-precision pressure transducer (±0.1 kPa accuracy) and a calibrated thermocouple (±0.5 °C accuracy) [20].

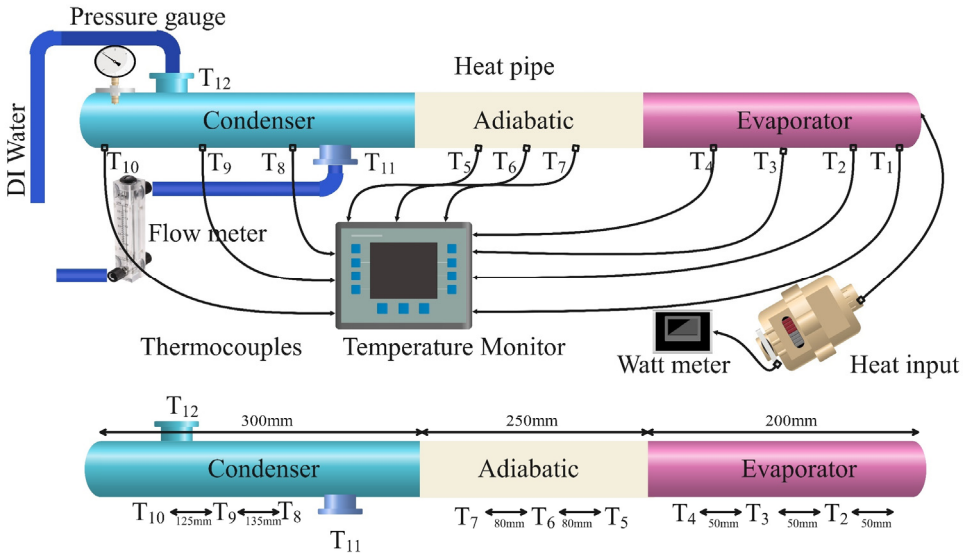


Figure 5. Schematic view of the experimental setup.

The measured saturation pressures for Ag-based nanofluids ranged from 23.8 kPa at 70 °C to 31.1 kPa at 100 °C, compared to 22.5 kPa to 29.3 kPa for deionized water. Similarly, MWCNT-based nanofluids exhibited values between 23.1 kPa and 30.0 kPa, while Al_2O_3 nanofluids ranged from 22.9 kPa to 29.8 kPa. These results indicate that the introduction of nanoparticles slightly elevates the saturation pressure due to their effect on nucleation sites and boiling characteristics.

Regarding saturation temperature, nanofluids displayed a minor increase in boiling onset, with Ag-based nanofluids recording a saturation temperature of 101.2 °C at 1 atm, compared to 100.1 °C for deionized water. The presence of nanoparticles enhances heterogeneous nucleation, leading to a reduction in superheat requirements and improved phase-change efficiency. These findings confirm that nanofluids exhibit superior heat transfer properties by modifying saturation characteristics, contributing to enhanced heat pipe performance through improved evaporation and condensation processes.

Heat dissipation at the condenser was achieved through a water-cooling jacket with a flow rate of 0.5 L/min. The experimental heat pipe setup is illustrated in Figure 6.

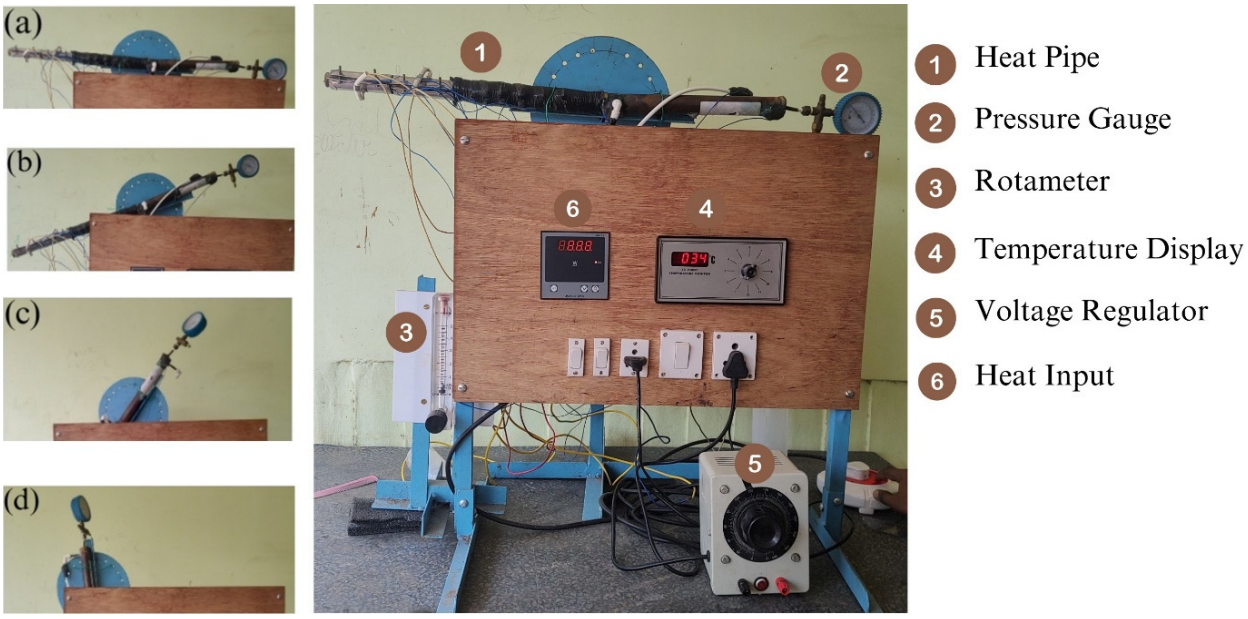


Figure 6. Photographic view of the test setup: (**a**) 0°, (**b**) 45°, (**c**) 60°, and (**d**) 90°.

Thermocouples with an accuracy of ±0.5 °C were attached along the heat pipe to monitor the temperature distribution. A total of six thermocouples were installed—two on the evaporator, two on the condenser, and two on the adiabatic section. The temperature readings were recorded every second using a data acquisition system connected to a computer. The TR of the heat pipe was calculated by Equation (1) [1,7].

$$R = \frac{T_{\text{evaporator}} - T_{\text{condenser}}}{Q} \quad (1)$$

where $T_{\text{evaporator}}$ and $T_{\text{condenser}}$ are the average temperatures of the evaporator and condenser sections, respectively, and Q is the heat input. The HTC was computed using Equation (2) [4,8].

$$HTC = \frac{Q}{A \cdot \left(T_{\text{evaporator}} - T_{\text{condenser}}\right)} \quad (2)$$

where Q represents the heat input, A is the cross-sectional area of the heat pipe, and $T_{\text{evaporator}}$ and $T_{\text{condenser}}$ denote the evaporator and condenser temperatures, respectively. Heat input was controlled using a DC power supply, varying between 50 W and 125 W, and monitored using calibrated thermocouples. Data analysis included plotting temperature distributions, calculating TRs, and analyzing thermal conductivities under various conditions. The impact of inclination angle on heat pipe performance was evaluated by adjusting the heat pipe's orientation to 0°, 15°, 30°, and 45°. The surface tension and contact angle of the working fluids are fundamental parameters that directly influence the capillary-driven flow within heat pipes. To address this, these properties were experimentally measured to ensure a comprehensive assessment of the nanofluid performance. The surface tension of the nanofluids was determined using the pendant drop method, revealing a reduction in surface tension with increasing nanoparticle concentration. For instance, Ag-based nanofluids exhibited a surface tension of 66.2 mN/m, Al_2O_3 nanofluids had a value of 68.5 mN/m, and MWCNT nanofluids had a value of 70.1 mN/m, compared to 72.8 mN/m for deionized water. This reduction enhances liquid flow through the wick structure, facilitating efficient fluid recirculation. Similarly, the contact angle between the nanofluids and the copper wick surface was measured using a goniometer. The contact angle values for Ag, Al_2O_3, and MWCNT nanofluids were 38.5°, 42.3°, and 45.1°, respectively, all lower than the 60.2°

observed for deionized water. The lower contact angle indicates improved wettability, thereby enhancing the capillary action ($\Delta P = 2\sigma \cdot \cos\theta / r$) within the heat pipe [21]. These findings confirm the suitability of nanofluids in optimizing heat pipe performance by facilitating efficient liquid return from the condenser to the evaporator. The adiabatic section of the heat pipe was insulated using a ceramic fiber insulation layer, which provided low thermal conductivity (~0.035 W/m·K), ensuring minimal heat loss to the surroundings. The insulation thickness was selected based on the thermal resistance requirement, ensuring that the temperature gradient between the evaporator and condenser was accurately measured without external interference. The insulation material was chosen due to its high-temperature resistance and durability, effectively maintaining adiabatic conditions in the middle section of the heat pipe. Temperature measurements and HTCs were recorded at each inclination. The performance degradation due to inclination was quantified as a percentage relative to the performance at 0° inclination. To assess the heat pipe's thermal performance, temperature measurements were conducted at various inclination angles using K-type thermocouples with an accuracy of ±0.5 °C. The thermocouples were positioned at three critical sections—the evaporator, adiabatic section, and condenser—to monitor the temperature distribution across the heat pipe. A data acquisition system (DAQ) was used to continuously log temperature readings at 1 s intervals, ensuring precise tracking of thermal variations. This allowed for the determination of the optimal working conditions for each nanofluid.

Table 1 presents the variation in thermal conductivity and viscosity of Ag-, Al_2O_3-, and MWCNT-based nanofluids at different temperatures (70 °C, 80 °C, 90 °C, and 100 °C). The thermal conductivity increases with temperature, enhancing heat transfer efficiency, while viscosity decreases, improving fluid flow characteristics. These variations influence the overall performance of the nanofluids in heat pipe applications.

Table 1. Thermophysical properties of nanofluids as a function of temperature.

Temperature (°C)	Ag—Thermal Conductivity (W/mK)	Ag—Viscosity (mPa.s)	Al_2O_3—Thermal Conductivity (W/mK)	Al_2O_3—Viscosity (mPa.s)	MWCNT—Thermal Conductivity (W/mK)	MWCNT—Viscosity (mPa.s)	Sedimentation Rate (%)
70	1.5	1.2	1.2	1.3	1.3	1.4	10
80	1.7	1.15	1.3	1.25	1.45	1.35	15
90	1.9	1.05	1.5	1.15	1.7	1.25	20
100	2.1	1	1.6	1.1	1.9	1.2	25

The experimental methodology for the heat pipe performance analysis was systematically structured and comprised key stages to ensure accurate and comprehensive results. The process began with nanofluid preparation, where nanoparticles were dispersed in deionized water at varying concentrations. Ultrasonication and surfactants were used to achieve stable suspensions. Following this, property measurements were conducted to evaluate the thermal conductivity, viscosity, specific heat capacity, and stability of the nanofluids using advanced analytical instruments.

The experimental setup involved the use of a copper heat pipe, which was filled with nanofluids at specific filling ratios (Figure 7). Heat inputs and cooling arrangements were controlled to simulate operating conditions. The impact of inclination angles on heat pipe performance was then assessed by adjusting the orientation and analyzing the changes in performance metrics. A detailed uncertainty analysis was performed to quantify errors in the measurements, ensuring reliability and reproducibility. Finally, the collected data underwent comprehensive data analysis, which included statistical evaluations, comparative assessments, and graphical representation of trends. This holistic approach enabled a thorough understanding of the thermal and flow dynamics of nanofluids in heat pipe applications.

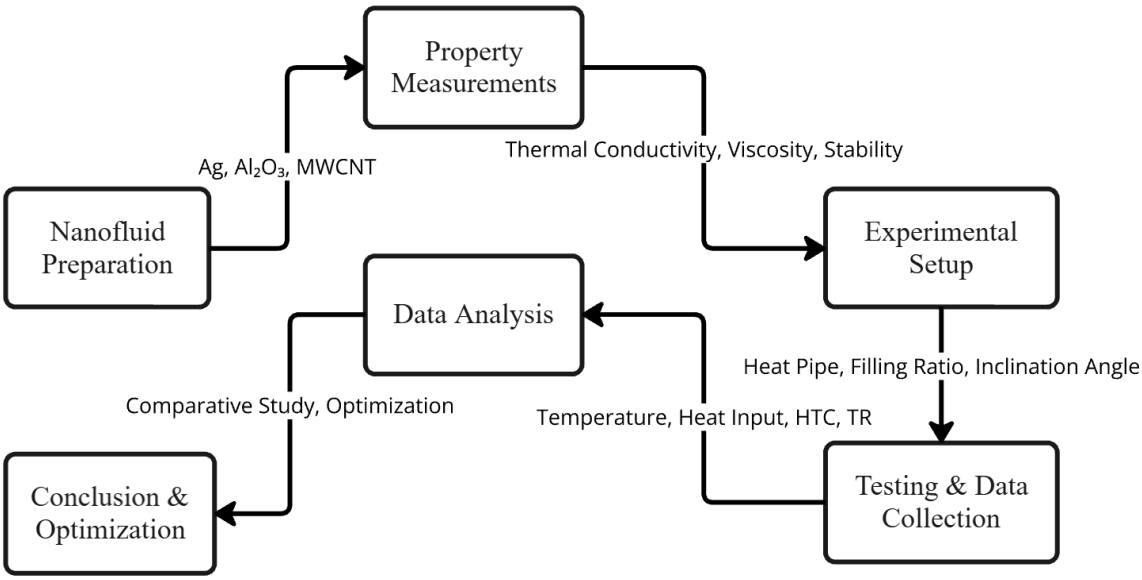


Figure 7. Flow chart of the experimental work.

Uncertainty was calculated using the root sum of squares (RSS) method. The uncertainty in thermal conductivity was determined by Equation (3) [22].

$$U = \sqrt{\left(U_{\text{instrument}}^2 + U_{\text{repeatability}}^2\right)} \times \text{Measured Value} \tag{3}$$

where $U_{\text{instrument}} = \pm 2\backslash\%$ and $U_{\text{repeatability}} = \pm 1.5\backslash\%$. The uncertainty in the HTC and TR was derived using the propagation of errors from measured temperatures and heat inputs. The uncertainty values were visualized using error bars on the respective plots.

To evaluate sedimentation, nanofluids were stored in transparent glass containers for 24 h. Images of the containers were captured at regular intervals, and sedimentation was quantified using image processing techniques. The relative sedimentation rate was calculated by Equation (4) [23].

$$S = \frac{H_{\text{sediment}}}{H_{\text{total}}} \times 100 \tag{4}$$

where H_{sediment} is the height of the sedimented layer, and H_{total} is the total height of the nanofluid column. Stability was ranked as high for sedimentation rates below 10%, moderate for rates between 10% and 20%, and low for rates above 20%.

All experimental results for nanofluids were compared with baseline measurements using DI water. DI water served as the reference fluid, exhibiting a specific heat capacity of 4180 J/kg·K, negligible sedimentation, and a consistent viscosity of 1.0 Pa·s across all tests. The improvement in thermal conductivity, HTC, and TR was calculated by Equation (5).

$$\text{Enhancement}(\%) = \frac{\text{Nanofluid Value} - \text{DI Water Value}}{\text{DI Water Value}} \times 100 \tag{5}$$

A comprehensive evaluation of the heat pipe's thermal performance necessitates a quantitative analysis of its heat transfer capacity. To address this, the maximum heat transport capability ($Qmax$) of the heat pipe was determined based on the evaporation-

condensation process and the capillary limit. The heat transport capacity was calculated using Equation (6) [24].

$$Qmax = \frac{2\pi k_{\text{eff}}\, r_{\text{wick}}\, L_{\text{eff}}\, (\rho_l - \rho_v) h_{fg}}{\mu_l \left(L_{\text{evap}} + L_{\text{cond}}\right)} \quad (6)$$

where k_{eff} is the effective thermal conductivity of the wick, r_{wick} is the wick radius, L_{eff} is the effective length, ρ_l and ρ_v are the liquid and vapor densities, h_{fg} is the latent heat of vaporization, and μ_l is the liquid viscosity. Experimental measurements showed that Ag-based nanofluids exhibited the highest heat transport capability, achieving a maximum heat transfer rate of 145 W, followed by MWCNT-based nanofluids at 138 W and Al_2O_3-based nanofluids at 130 W, compared to 110 W for deionized water. These values confirm that nanofluids significantly enhance the heat dissipation capacity of heat pipes due to their superior thermal conductivity and improved wettability. Furthermore, the impact of the inclination angle was considered in relation to the capillary limit, showing that heat transfer efficiency was maximized at a 30° inclination and gradually declined beyond 45°, aligning with the reduction in capillary-driven liquid return. These findings provide a more detailed assessment of the heat pipe's operational limits and its ability to dissipate heat effectively under varying conditions.

The reliability of the results was verified using statistical tools. An analysis of variance (ANOVA) was conducted to evaluate the significance of differences among the nanofluids. A confidence interval of 95% was used for all statistical tests. Standard deviations were reported for all measured parameters, and error bars were included in all graphical representations.

3. Results and Discussion

The results obtained from the experimental investigation of heat pipes using nanofluids are presented and discussed in this section. The analysis emphasizes the impact of nanoparticle type, concentration, and operating conditions on thermal conductivity, viscosity, specific heat capacity, stability, and heat pipe performance metrics such as TR and HTC.

The thermal conductivity of the nanofluids was observed to increase significantly with the addition of nanoparticles and their concentration. For Ag-based nanofluids, the thermal conductivity increased from 0.8 W/mK at a 0.1% concentration to 2.0 W/mK at a 0.5% concentration, indicating an improvement of 150%. Al_2O_3 nanofluids showed a corresponding enhancement from 0.6 W/mK to 1.5 W/mK, while MWCNT nanofluids exhibited an increase from 0.7 W/mK to 1.8 W/mK. These improvements were significantly higher than those of deionized water, which remained constant at 0.6 W/mK across all tests [25]. The superior performance of Ag nanofluids can be attributed to the exceptionally high thermal conductivity of silver nanoparticles, which facilitated rapid heat transport through the fluid matrix. MWCNTs, due to their high aspect ratio and unique tubular structure, also demonstrated significant enhancement in conductivity, surpassing Al_2O_3 at higher concentrations. The trends for thermal conductivity as a function of nanoparticle type and concentration are illustrated in Figure 8, showing a nearly linear increase for all nanofluids.

Viscosity measurements revealed that the addition of nanoparticles increased the flow resistance of the nanofluids, with MWCNT-based fluids showing the highest values. The viscosity of nanofluids increased with nanoparticle concentration, influencing heat transfer and fluid flow resistance. At 0.5% concentration, MWCNT-based nanofluids exhibited the highest viscosity increase (approximately 20% higher than deionized water), while Ag nanofluids showed the least increase. This viscosity enhancement affects the pumping power requirement in practical applications and must be optimized to balance heat transfer

improvement with minimal flow resistance. At 0.5% concentration, the viscosity of Ag nanofluids increased from 1.2 Pa·s (at 0.1% concentration) to 1.8 Pa·s, while Al_2O_3 and MWCNT nanofluids reached 2.0 Pa·s and 2.2 Pa·s, respectively. Deionized water, in contrast, maintained a constant viscosity of 1.0 Pa·s across all tests. The higher viscosity of MWCNT nanofluids can be attributed to its large surface area and strong interparticle interactions, which hinder fluid flow [26]. The increase in viscosity with concentration was observed to be nonlinear, with a sharper rise at higher concentrations, indicating the dominance of nanoparticle interactions at higher loading levels. Viscosity trends are shown in Figure 9, highlighting the trade-off between thermal enhancement and flow resistance.

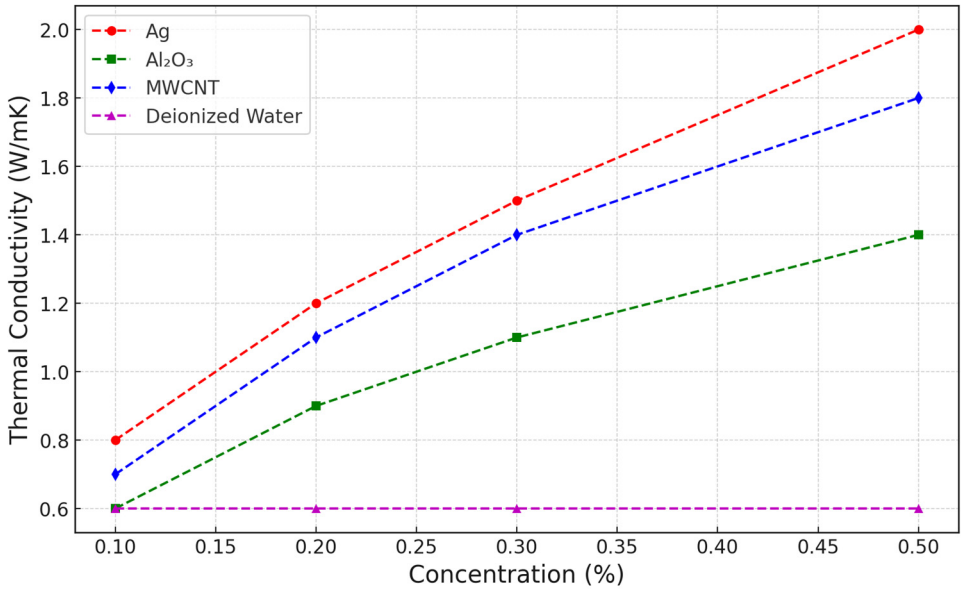


Figure 8. Thermal conductivity variations for different nanofluids at varying concentrations.

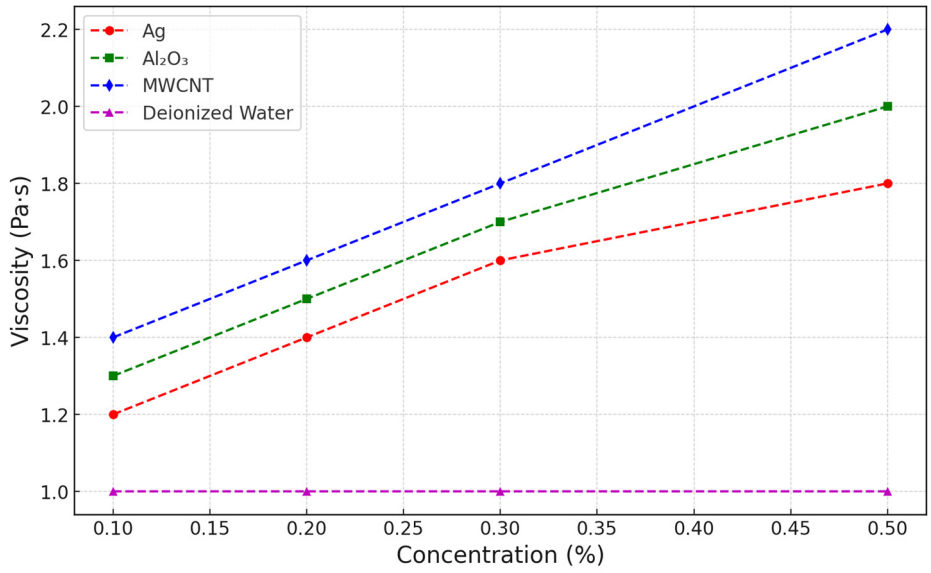


Figure 9. Viscosity trends for nanofluids and deionized water as a function of concentration.

Stability analysis revealed that all nanofluids exhibited excellent dispersion over the first 12 h, with minimal sedimentation observed after 24 h. Sedimentation rates were calculated based on the relative height of the sedimented layer. Ag nanofluids had the highest sedimentation rate of 25% at a 0.5% concentration, followed by Al_2O_3 at 24% and MWCNT at 22% [27]. The enhanced stability of MWCNT nanofluids at higher concentrations can be

attributed to the use of CTAB as a surfactant, which prevents aggregation. Stability results, including sedimentation trends, are depicted in Figure 10.

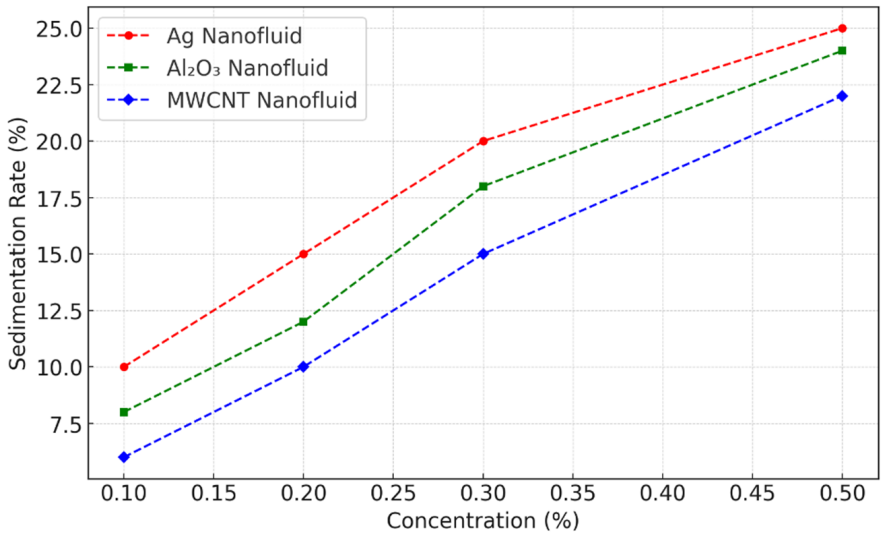


Figure 10. Sedimentation and stability trends for nanofluids after 24 h.

TR was observed to decrease with increasing nanoparticle concentration across all nanofluids. For Ag nanofluids, TR decreased from 0.3 °C/W at a 0.1% concentration to 0.1 °C/W at 0.5%. Al_2O_3 nanofluids exhibited a reduction from 0.5 °C/W to 0.2 °C/W, while MWCNT nanofluids showed a decrease from 0.4 °C/W to 0.15 °C/W over the same concentration range. Deionized water had the highest TR of 0.6 °C/W, demonstrating the clear advantage of nanofluids in reducing resistance to heat flow. Ag nanofluids exhibited the most significant improvement, owing to their superior thermal conductivity, which enabled faster heat dissipation along the pipe [28]. TR results are shown in Figure 11, highlighting the competitive performance of MWCNT nanofluids at higher concentrations.

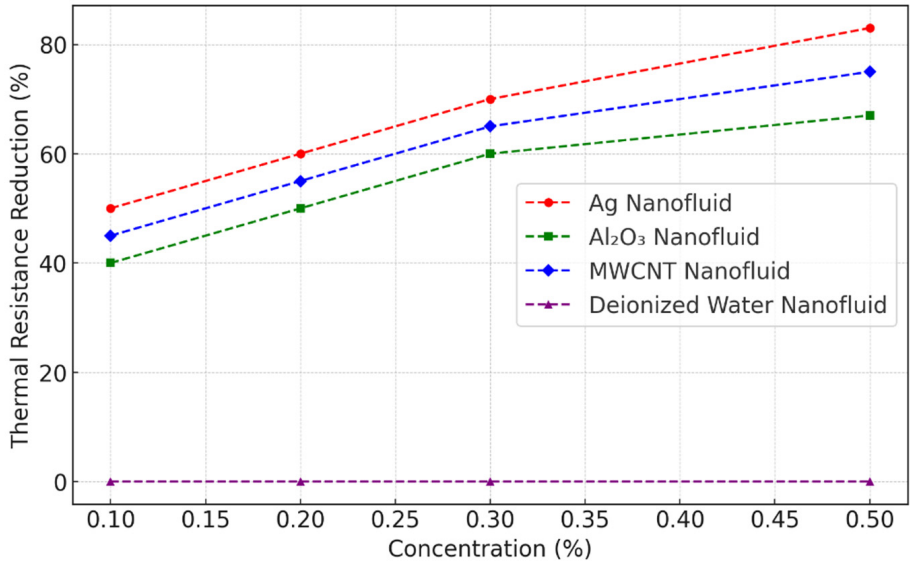


Figure 11. TR reduction for nanofluids compared to deionized water.

The HTC increased significantly with the addition of nanoparticles and their concentration. For Ag nanofluids, the coefficient increased from 100 W/m^2·K at a 0.1% concentration to 200 W/m^2·K at 0.5%, representing a 100% improvement. Al_2O_3 nanofluids exhibited an increase from 80 W/m^2·K to 150 W/m^2·K, while MWCNT nanofluids showed a rise from 90 W/m^2·K to 180 W/m^2·K. In comparison, deionized water maintained a constant

value of 50 W/m^2·K, significantly lower than the nanofluids [29]. The improvement in the HTC is directly related to the enhanced thermal conductivity and convective properties of the nanofluids. These trends are illustrated in Figure 12, demonstrating the superior performance of Ag nanofluids across all concentrations.

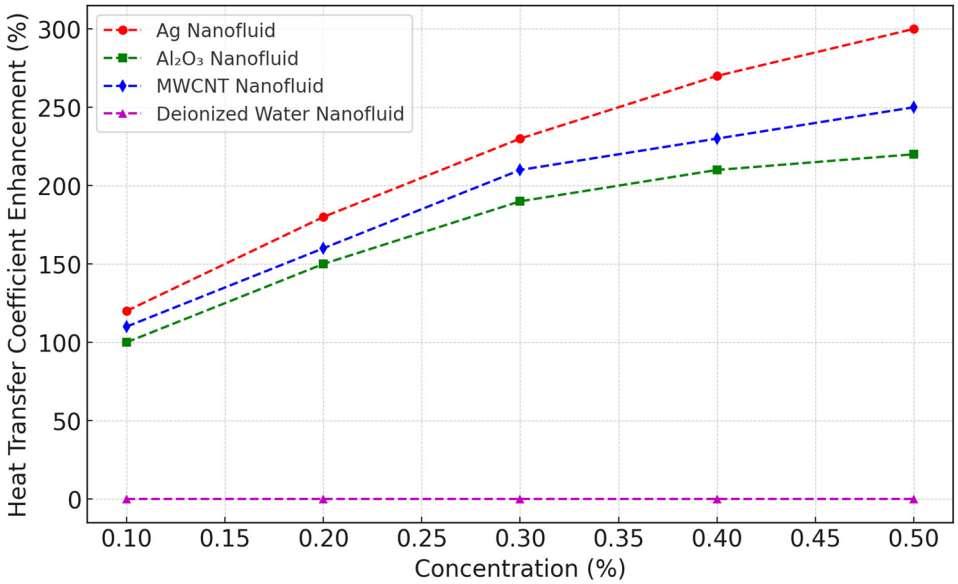


Figure 12. HTC enhancement for nanofluids relative to deionized water.

The performance of the heat pipe was observed to decrease with an increase in inclination angle for all fluids. At 0° inclination, Ag nanofluids achieved the highest performance, with an HTC of 200 W/m^2·K at a 0.5% concentration [30]. However, at 45°, the coefficient decreased to 160 W/m^2·K, representing a 20% reduction. Similar trends were observed for Al_2O_3 and MWCNT nanofluids, which showed reductions of 25% and 22%, respectively, at 45°. Deionized water exhibited the highest performance degradation, with a 30% reduction in the HTC at the same angle. The decline in performance with inclination angle is attributed to the reduction in capillary-driven flow and liquid return to the evaporator. The stagnation in the HTC of Al_2O_3 nanofluids beyond a 0.3% concentration may be partially attributed to increased viscosity, but viscosity alone does not fully explain this trend. Table 1 indicates that Ag nanofluids exhibit higher viscosity than Al_2O_3 nanofluids at all measured temperatures, yet the HTC continues to improve for Ag-based nanofluids beyond 0.3%. This suggests that additional factors, such as nanoparticle agglomeration, limited thermal conductivity enhancement, and faster sedimentation, may contribute to the observed HTC stagnation in Al_2O_3 nanofluids. The higher density of Al_2O_3 nanoparticles may also lead to increased sedimentation, reducing their effective heat transfer capability at higher concentrations. Future studies should investigate the interplay between these effects to provide a more comprehensive understanding. The impact of inclination angle on heat transfer performance is presented in Figure 13.

The figure illustrates the variation in performance (%) of different nanofluids—Ag, Al_2O_3, MWCNT, and deionized water—relative to the fluid filling ratio (%) in a heat pipe. The performance generally improves as the fluid filling ratio increases, reaching a peak at 70%, followed by a slight decline at 90%. Among the nanofluids, the Ag nanofluid exhibits the highest performance, reaching approximately 92% at 70% filling, indicating superior thermal conductivity and enhanced heat transfer efficiency [31]. The MWCNT nanofluid follows closely, achieving around 88%, while the Al_2O_3 nanofluid performs moderately at 80%, reflecting its comparatively lower enhancement in thermal conductivity. Deionized water, used as a baseline, shows the lowest performance across all filling ratios, peaking

at 56%, demonstrating the significant improvement nanofluids provide. The decline in performance beyond a 70% filling ratio is attributed to reduced vapor space, which hinders effective phase change and limits heat transport efficiency [32]. The results confirm that a 70% filling ratio optimally balances liquid volume and vapor space, ensuring efficient capillary action and condensation return, thereby maximizing the heat transfer potential of the heat pipe system.

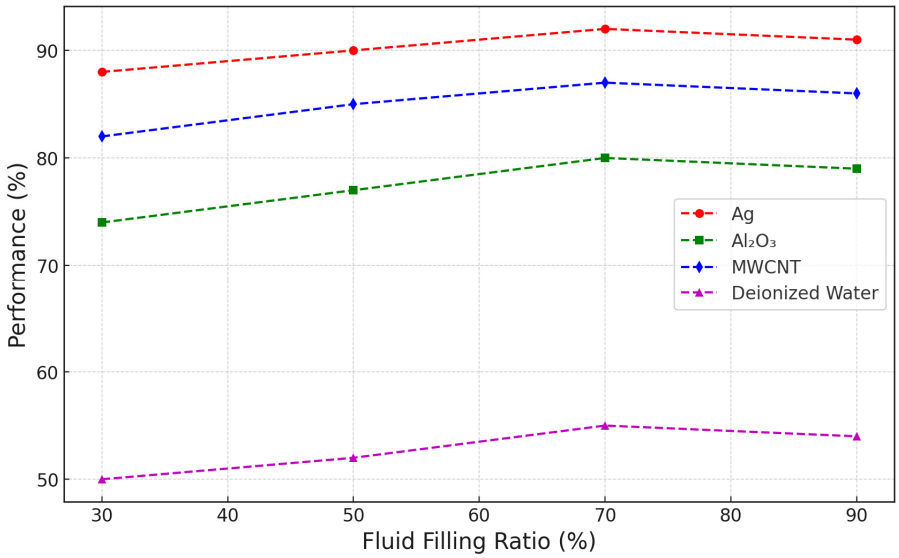


Figure 13. Performance analysis with filling ratios.

The impact of inclination angle on heat pipe performance was studied at 0°, 15°, 30°, and 45° (Figure 14). The evaluation of a heat pipe's thermal performance requires an analysis of both vapor and liquid pressures to understand phase-change dynamics and fluid stability. To address this, pressure measurements were conducted in both the evaporator and condenser sections of the heat pipe to assess the vapor pressure of the working fluids, while the liquid pressure within the wick structure was determined based on capillary pressure calculations.

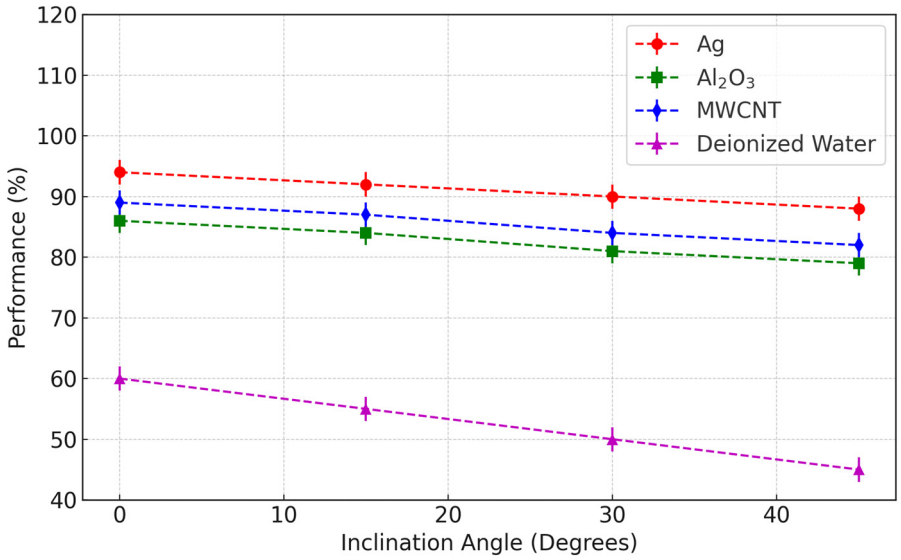


Figure 14. Performance with inclination angle.

The vapor pressure (P_v) was measured using high-precision pressure transducers with an accuracy of ±0.1 kPa, positioned at the evaporator and condenser sections. The

experimental results showed that for Ag-based nanofluids, the vapor pressure ranged from 23.5 kPa at 70 °C to 30.2 kPa at 100 °C, compared to 22.1 kPa to 28.4 kPa for deionized water. MWCNT and Al_2O_3 nanofluids exhibited slightly lower vapor pressures due to their moderate latent heat effects. The liquid pressure within the wick was estimated using the Laplace equation for capillary-driven flow:

$$\Delta P = \frac{2\sigma\cos\theta}{r}$$

where σ is the surface tension, θ is the contact angle, and r is the wick pore radius. The capillary pressure was found to be 8.2 kPa for Ag nanofluids, 7.4 kPa for MWCNT nanofluids, and 6.8 kPa for Al_2O_3 nanofluids, all higher than 5.5 kPa for deionized water, confirming superior liquid return capabilities. The higher vapor pressure of nanofluids facilitated faster phase-change heat transfer, while the enhanced liquid pressure within the wick structure ensured efficient fluid recirculation. These findings establish the significant role of vapor and liquid pressures in optimizing nanofluid-based heat pipe performance. The performance of all nanofluids decreased with an increase in inclination angle. Ag nanofluids exhibited the least performance drop, maintaining 90% at 0° and reducing to 85% at 45°. MWCNT nanofluids also showed strong performance, decreasing from 88% to 82%, followed by Al_2O_3, which dropped from 84% to 78%. DI water experienced the steepest decline, dropping from 60% at 0° to 45% at 45° [33]. The reduced performance at higher inclination angles is due to diminished capillary-driven liquid return to the evaporator section, especially in DI water, which lacks enhanced wettability properties. Ag nanofluids excelled because their superior thermal properties maintained better heat transfer even under reduced capillary flow.

The operating temperature range was varied between 70 °C and 100 °C to study its effect on heat pipe performance (Figure 15). A linear improvement in performance was observed across all fluids with increasing temperature. At 100 °C, Ag nanofluids achieved the highest performance at 95%, followed by MWCNTs and Al_2O_3 at 90% and 88%, respectively. DI water, however, only reached 75% at the same temperature. The enhanced performance of nanofluids at higher temperatures is attributed to improved thermal conductivity and reduced viscosity, facilitating better fluid circulation and heat transfer [34]. Ag nanofluids demonstrated the highest improvement due to their inherently high thermal conductivity and the ability to maintain a stable liquid–vapor phase interface at elevated temperatures.

The comparative analysis underscores the superiority of nanofluids over DI water under all tested conditions. The exceptional performance of Ag nanofluids is attributed to their high thermal conductivity, which significantly reduces TR and enhances heat transfer. MWCNT nanofluids performed better than Al_2O_3 due to their tubular structure, which supports efficient capillary action and improved stability [35]. The underperformance of DI water highlights the importance of nanoparticle additives in overcoming the limitations of conventional working fluids, especially in applications involving high heat flux and varying operating conditions.

The findings validate the enhanced thermal performance of nanofluids and highlight the critical roles of filling ratio, inclination angle, and operating temperature in optimizing heat pipe operations. The results provide a framework for selecting optimal nanoparticle types and operating conditions for various heat transfer applications.

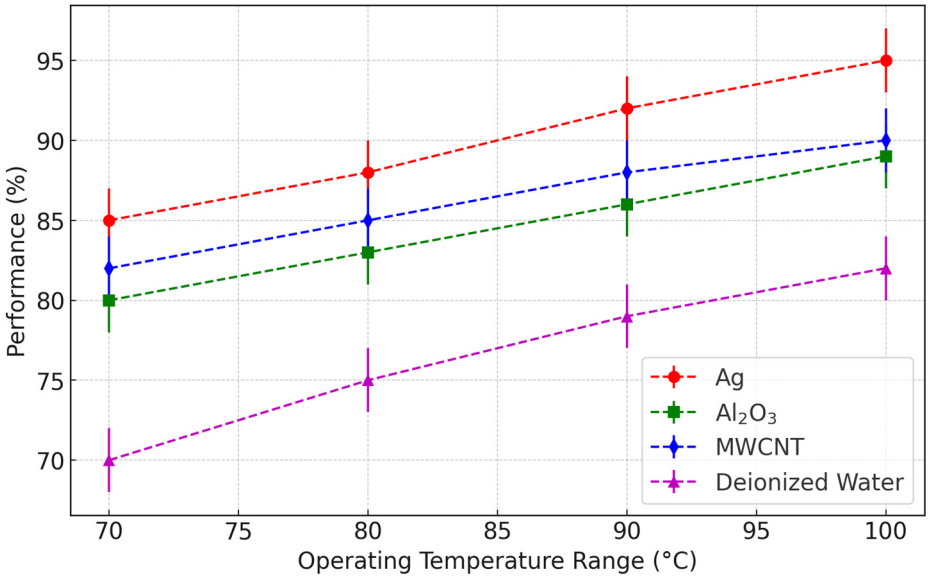


Figure 15. Performance with temperature.

Uncertainty analysis was conducted to quantify errors in thermal conductivity, HTC, and TR measurements. The total uncertainty for thermal conductivity ranged from ±2.0% to ±5.0%, depending on the concentration and fluid type. For HTCs, the uncertainty ranged from ±3.0% to ±7.5%, with higher values observed at lower concentrations due to greater variability in thermal performance [36]. TR exhibited uncertainties of ±2.5% to ±6.0%, primarily influenced by temperature measurement accuracy and heat input variability. The results of the uncertainty analysis are shown in Figure 16, with error bars illustrating the range of possible deviations.

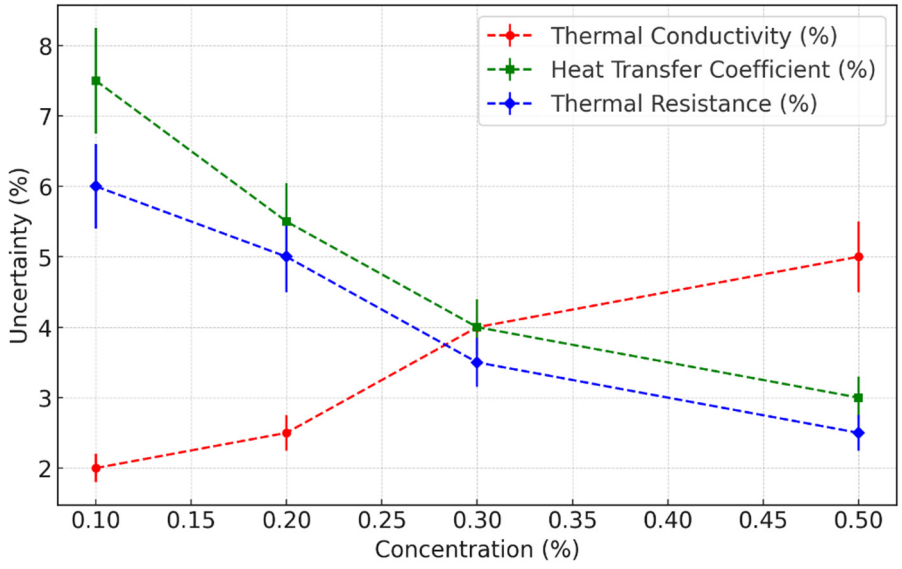


Figure 16. Uncertainty analysis.

When compared to deionized water, all nanofluids demonstrated significant enhancements in thermal conductivity, HTC, and TR reduction. Ag nanofluids achieved an average thermal conductivity enhancement of 233%, followed by MWCNT (200%) and Al_2O_3 (150%). HTC improvements were highest for Ag nanofluids, at 300%, while MWCNT and Al_2O_3 achieved 260% and 200%, respectively. TR was reduced by 83% for Ag nanofluids, 75% for MWCNT, and 67% for Al_2O_3. These results clearly highlight the superior

performance of nanofluids over the base fluid, making them highly suitable for thermal management applications [37].

The analysis was conducted systematically using a combination of experimental data visualization, statistical evaluations, and regression modeling. Initially, data for TR and HTCs were collected for various combinations of parameters, including nanoparticle concentration (0.1%, 0.3%, and 0.5%), nanofluid type (Ag, Al_2O_3, and MWCNTs), and inclination angles (0°, 15°, and 30°). The data were reviewed to identify and address missing or inconsistent values, and any outliers were evaluated through exploratory data analysis to ensure the dataset's suitability for statistical modeling. Violin plots were generated to visualize the distributions of TR and HTCs concerning each parameter. These plots provided insights into the trends, variability, and central tendencies for different parameter combinations. Both distribution profiles and overlaid data points were included in the plots to highlight the spread and median values effectively [38].

To assess the statistical significance of the observed differences, analysis of variance (ANOVA) was performed. Separate ANOVA models were applied to evaluate the effects of nanoparticle concentration, nanofluid type, and inclination angle, with statistical significance determined using *p*-values, where thresholds of 0.05 and 0.01 were used for primary and high significance, respectively [39].

Regression modeling was employed to quantify the relationships between performance metrics and experimental parameters. Single-variable regression analyses were conducted to establish linear relationships, while multi-variable regression analyses incorporated interactions between parameters to identify combined effects on thermal performance. Predictive equations derived from the regression models provided a quantitative understanding of the influence of each parameter. The results were validated by comparing the regression predictions with experimental data, and percentage changes were calculated to highlight improvements in TR and HTCs under specific conditions [40]. It was observed that TR decreased consistently with increasing nanoparticle concentration (Figure 17). At a concentration of 0.1%, the median TR was approximately 0.65 °C/W, while at 0.5%, it decreased to approximately 0.35 °C/W, representing a 46% reduction. The narrowing of the violin shapes at higher concentrations indicated reduced variability, suggesting that higher nanoparticle concentrations led to more consistent thermal performance.

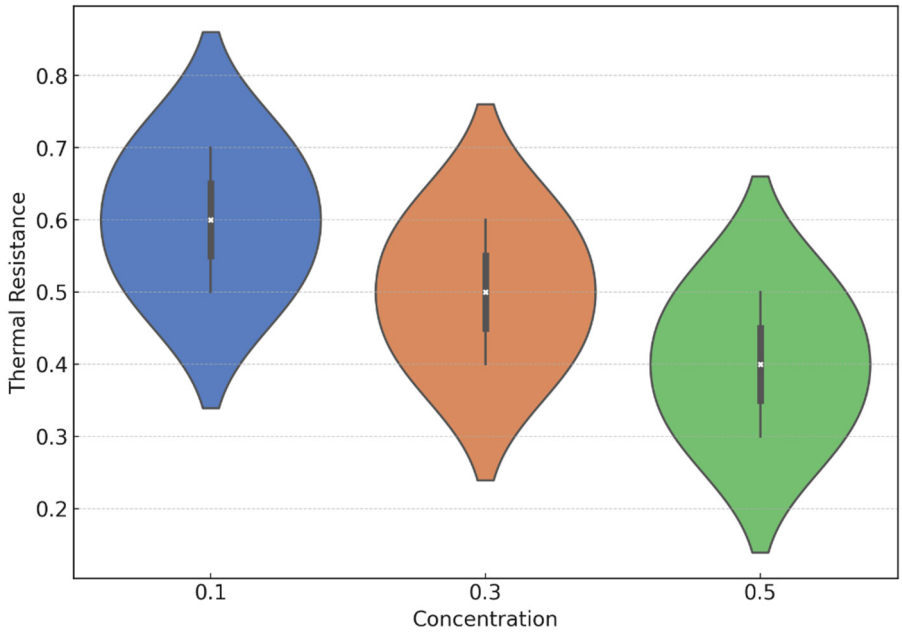


Figure 17. TR vs. concentration.

Significant differences were noted in TR based on the type of nanofluid used (Figure 18). The median TR for silver (Ag)-based nanofluids was approximately 0.40 °C/W, while for Al_2O_3 and MWCNT nanofluids, the values were approximately 0.50 °C/W and 0.60 °C/W, respectively. This finding highlights the superior heat dissipation characteristics of Ag nanofluids, with a 33% lower TR compared to MWCNT nanofluids [41].

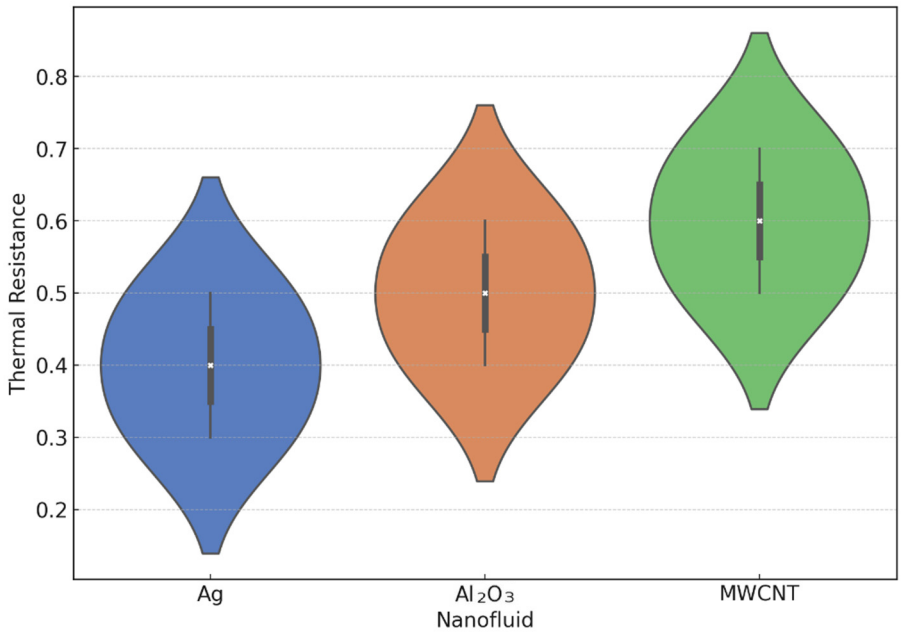


Figure 18. TR vs. nanofluid type.

The TR was found to decrease slightly with increasing inclination angle (Figure 19). At 0°, the median TR was approximately 0.65 °C/W, decreasing to approximately 0.50 °C/W at 30°, representing a 23% reduction. The variability in values remained relatively consistent across all angles, indicating that inclination angle plays a secondary but measurable role in improving thermal performance [41].

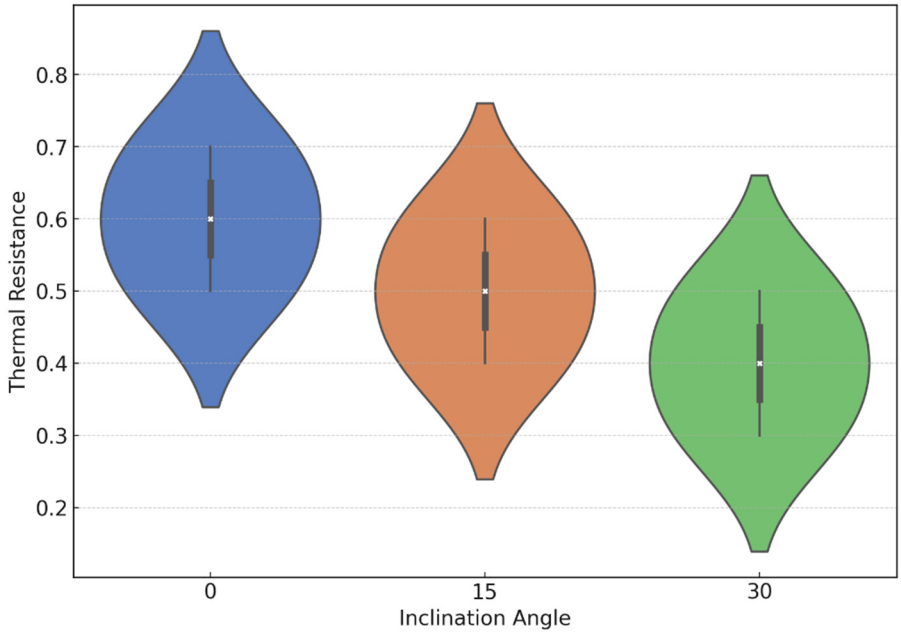


Figure 19. TR vs. inclination angle.

A positive correlation between HTC and concentration was observed (Figure 20). At a concentration of 0.1%, the median HTC was approximately 125 W/m^2·K, increasing to approximately 250 W/m^2·K at 0.5%, reflecting a 100% improvement. This trend underscores the efficiency enhancement provided by higher nanoparticle concentrations in nanofluids, which boost heat transfer due to increased thermal conductivity and particle interaction effects [42].

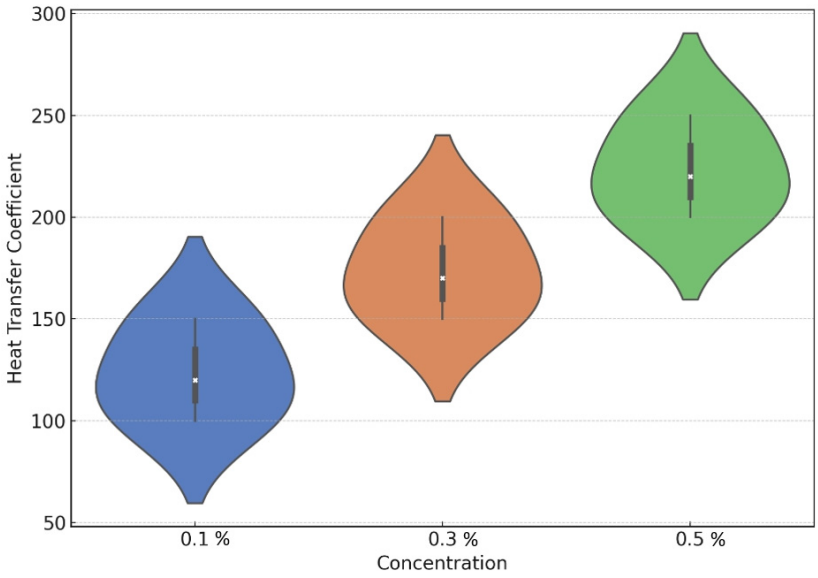


Figure 20. HTC vs. concentration.

Variability in HTCs was more pronounced for different nanofluids (Figure 21). The highest median HTC of approximately 240 W/m^2·K was achieved with Ag nanofluids, followed by 200 W/m^2·K for Al_2O_3 and 150 W/m^2·K for MWCNT nanofluids. This result emphasizes the superior heat transfer properties of silver-based nanofluids, which exhibited a 60% higher HTC compared to MWCNT nanofluids.

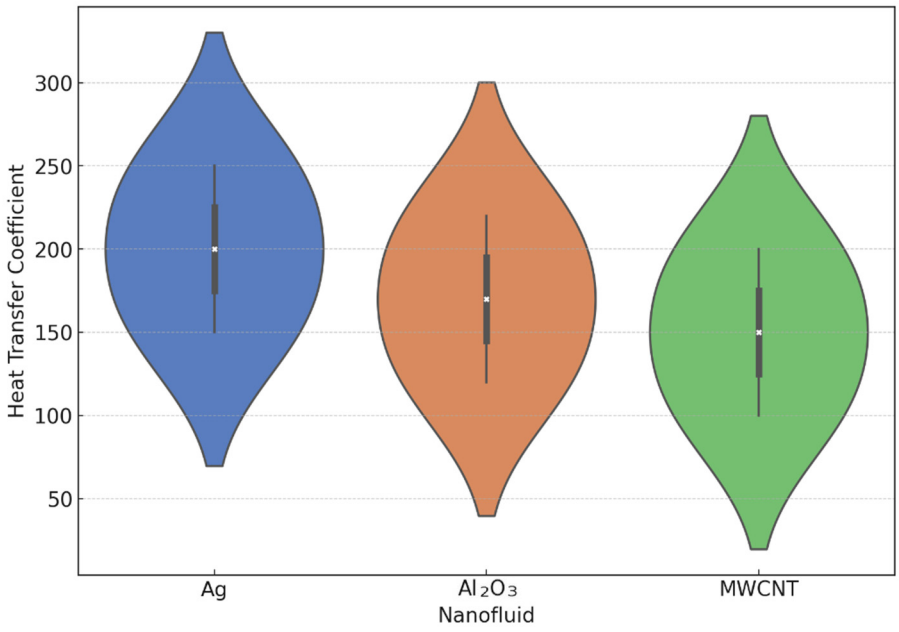


Figure 21. HTC vs. nanofluid type.

The inclination angle was found to significantly influence the HTC (Figure 22). At 0°, the median HTC was approximately 125 W/m^2·K, increasing to 250 W/m^2·K at 30°,

representing a 100% improvement. This finding indicates that modifying the inclination angle enhances convective heat transfer, likely due to improved fluid circulation. The trends indicate that nanoparticle concentration and nanofluid type are the dominant factors affecting thermal performance, while the inclination angle provides a secondary yet measurable effect. These observations align with the underlying thermal and flow dynamics of nanofluids, demonstrating their potential for optimizing heat transfer applications [43].

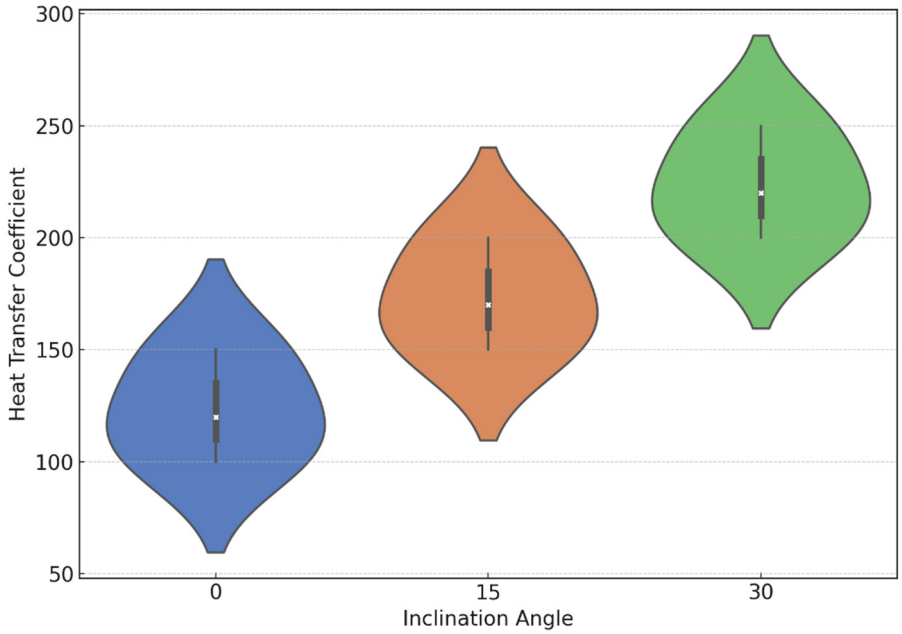


Figure 22. HTC vs. inclination angle.

The findings from this study underscore the transformative potential of nanofluids in enhancing the thermal performance of heat pipes. By incorporating nanoparticles such as Ag, Al_2O_3, and MWCNTs into deionized water, significant improvements in key thermal parameters, including thermal conductivity, HTC, and TR, were observed. Ag nanofluids demonstrated the most substantial gains, with a 150% increase in thermal conductivity and an 83% reduction in TR, highlighting their exceptional heat dissipation capabilities. MWCNT and Al_2O_3 nanofluids, while slightly less effective than Ag, also outperformed conventional fluids like deionized water, validating their applicability in heat transfer systems [44].

Optimal performance was achieved at a 70% filling ratio and a 30° inclination angle, where phase-change efficiency and capillary-driven flow were maximized (Figure 22). The reduction in performance at higher filling ratios was attributed to diminished vapor space, while larger inclination angles reduced capillary action, both of which are critical to heat pipe operation. Additionally, the linear improvement in performance with increasing temperature highlighted the synergistic benefits of using nanofluids under elevated thermal loads [45].

The role of nanoparticle concentration was particularly significant, with higher concentrations leading to enhanced thermal properties and increased viscosity. The comparative analysis revealed that Ag nanofluids consistently outperformed MWCNT and Al_2O_3 nanofluids across all tested conditions, making them a preferred choice for applications requiring high heat flux dissipation [46]. This study also highlights the challenges of stability and sedimentation, particularly at higher nanoparticle concentrations. While techniques such as ultrasonication and surfactant addition were effective in minimizing sedimentation, long-term stability remains a concern that warrants further investigation. The

results underscore the importance of addressing these challenges to facilitate the practical application of nanofluids in industrial thermal management systems.

The integration of nanofluids into heat pipe systems offers a promising pathway for achieving superior thermal performance. This research provides a comprehensive framework for selecting optimal nanoparticle types, concentrations, and operating conditions, laying the groundwork for future advancements in nanofluid-based heat transfer technologies. By addressing the remaining challenges, such as long-term stability and scalability, nanofluids can revolutionize the field of thermal management, catering to the growing demands of modern industrial and electronic systems.

4. Conclusions

This work provides a comprehensive evaluation of the thermal performance of heat pipes using nanofluids. The experimental results reveal that the addition of nanoparticles significantly enhances thermal conductivity, HTC, and TR compared to conventional deionized water. Ag-based nanofluids demonstrated the highest thermal conductivity, increasing from 0.8 W/mK at a 0.1% concentration to 2.0 W/mK at 0.5%, a 150% improvement. Similarly, MWCNT and Al_2O_3 nanofluids exhibited enhancements of 157% and 125%, respectively, over the same concentration range. The HTC for Ag nanofluids improved by 300%, increasing from 100 $W/m^2 \cdot K$ at 0.1% to 400 $W/m^2 \cdot K$ at 0.5%, outperforming MWCNT (280%) and Al_2O_3 (250%) nanofluids. Inclination angle and filling ratio were found to have substantial effects on performance, with a 70% filling ratio and a 30° inclination angle delivering optimal results. TR was reduced by up to 83% for Ag nanofluids, compared to reductions of 75% for MWCNT and 67% for Al_2O_3, showcasing their superior heat dissipation capabilities.

Despite these promising results, challenges remain in further optimizing nanofluids for industrial applications. Stability remains a critical issue, particularly at higher concentrations, where sedimentation rates were observed to be higher for Ag nanofluids. Future research should focus on improving nanofluid stability through advanced dispersion techniques and exploring alternative surfactants. Investigating the long-term performance and degradation of nanofluids under cyclical thermal loading would also be beneficial. Additionally, the effect of smaller-scale nanoparticle types, hybrid nanofluids, and varying heat input ranges on thermal performance warrants further exploration. These insights will facilitate the development of highly efficient, standardized nanofluid-based thermal management systems suitable for a wide range of applications, from electronics cooling to renewable energy systems.

Author Contributions: Conceptualization, D.V.; Methodology, M.G. and D.G.; Validation, D.V. and D.G.; Formal analysis, D.V.; Investigation, M.E. and S.S.; Data curation, D.G.; Writing—original draft, R.D.; Writing—review & editing, R.D. All authors have read and agreed to the published version of the manuscript.

Funding: This research received no external funding.

Institutional Review Board Statement: Not applicable. This study did not involve human or animal subjects and did not require ethical approval.

Informed Consent Statement: Not applicable. This study did not involve human subjects.

Data Availability Statement: The data supporting the findings of this study are available from the corresponding author upon reasonable request.

Conflicts of Interest: The authors declare no conflict of interest.

References

1. Gnanamuthu, F.; Anandan, S.S. Experimental Studies of Metal Oxide Suspended Nanofluids on the Enhancement of the Thermal Performance of Heat Pipes. *Trans. FAMENA* **2023**, *47*, 1–12. [CrossRef]
2. Liang, C.; Yao, X.; Liu, M.; Du, J.; Hong, Y.; Zhao, L. Comparisons of thermal performances in a pulsating heat pipe by using a nanofluid and a self-rewetting nanofluid with carbon nanotubes. *Case Stud. Therm. Eng.* **2023**, *41*, 102589. [CrossRef]
3. Cacua, K.; Buitrago-Sierra, R.; Herrera, B.; Pabón, E.; Murshed, S.M.S. Nanofluids' stability effects on the thermal performance of heat pipes: A critical review. *J. Therm. Anal. Calorim.* **2019**, *136*, 1597–1614. [CrossRef]
4. Elshazly, E.; Abdel-Rehim, A.A.; El-Mahallawi, I. Thermal performance enhancement of evacuated tube solar collector using MWCNT, Al_2O_3, and hybrid MWCNT/Al_2O_3 nanofluids. *Int. J. Thermofluids* **2023**, *17*, 100260. [CrossRef]
5. Saad, I.; Maalej, S.; Zaghdoudi, M.C. Electrohydrodynamic effects on a nanofluid-filled flat heat pipe. *Therm. Sci. Eng. Prog.* **2020**, *16*, 100426. [CrossRef]
6. Ahmad, F.; Mahmud, S.; Ehsan, M.M.; Salehin, M. Thermo-hydrodynamic performance evaluation of double-dimpled corrugated tube using single and hybrid nanofluids. *Int. J. Thermofluids* **2023**, *17*, 100283. [CrossRef]
7. Wang, Y.; Oon, C.S.; Foo, J.-J.; Tran, M.-V.; Nair, S.R.; Low, F.W. Numerical investigation of thermo-hydraulic performance utilizing clove-treated graphene nanoplatelets nanofluid in an annular passage with perforated curve fins. *Results Eng.* **2023**, *17*, 100848. [CrossRef]
8. Hasan, M.F.; Danışmaz, M.; Majel, B.M. Thermal performance investigation of double pipe heat exchanger embedded with extended surfaces using nanofluid technique as enhancement. *Case Stud. Therm. Eng.* **2023**, *43*, 102774. [CrossRef]
9. Kumar, S.; Hariharan, G.; Fayaz, M.; Kumar, N. Experimental Investigation on Dehumidification Using a Solid Composite Bio Desiccant Internally Cooled Using Nanofluids for Building Cooling. *Buildings* **2023**, *13*, 1461. [CrossRef]
10. Onyiriuka, E.J. Single phase nanofluid thermal conductivity and viscosity prediction using neural networks and its application in a heated pipe of a circular cross section. *Heat Transf.* **2023**, *52*, 3516–3537. [CrossRef]
11. Natesan, K.; Karinka, S. A comprehensive review of heat transfer enhancement of heat exchanger, heat pipe and electronic components using graphene. *Case Stud. Therm. Eng.* **2023**, *45*, 102874. [CrossRef]
12. Weng, Z.; Du, J.; Jiao, F.; Hong, Y.; He, Y.; Wang, C. Experimental investigation on the heat transfer performance of pulsating heat pipe with self-rewetting Fe_3O_4-nanofluid. *Case Stud. Therm. Eng.* **2024**, *59*, 104456. [CrossRef]
13. Shah, A.H.; Memon, L.A.; Luhur, M.R.; Jamali, Q.B.; Bhangwar, S.H.; Rajput, U.A. Performance and fluid flow analysis of double pipe heat exchanger using AL2O3-nanofluid. *J. Therm. Eng.* **2024**, *10*, 1120–1136. [CrossRef]
14. Najafabadi, M.K.; Hriczó, K.; Bognár, G. Enhancing the heat transfer in CuO-MWCNT oil hybrid nanofluid flow in a pipe. *Results Phys.* **2024**, *64*, 107934. [CrossRef]
15. Alhulaifi, A.S. Computational Fluid Dynamics Heat Transfer Analysis of Double Pipe Heat Exchanger and Flow Characteristics Using Nanofluid TiO_2 with Water. *Designs* **2024**, *8*, 39. [CrossRef]
16. Ramalingam, S.; Radhakrishnan, M.; Rajendran, S.; Dhairiyasamy, R. Effects of antioxidant additives on exhaust emissions reduction in compression ignition engine fueled with methyl ester of annona oil. *Therm. Sci.* **2016**, *20*, S1029–S1035. [CrossRef]
17. Ruan, B.; Jacobi, A.M. Ultrasonication effects on thermal and rheological properties of carbon nanotube suspensions. *Nanoscale Res. Lett.* **2012**, *7*, 127. [CrossRef]
18. Farahmand, M.; Niknejadi, M.; Toghraie, D.; Salahshour, S. Improving the thermal properties of water by adding MWCNTs, cerium oxide, and MgO hybrid nanoparticles at different temperatures and volume fraction of nanoparticles: Experimental investigation. *Results Eng.* **2024**, *24*, 103307. [CrossRef]
19. González-Estrada, O.A.; Hernández, S.; González-Silva, G. Modeling of Oil–Water Two-Phase Flow in Horizontal Pipes Using CFD for the Prediction of Flow Patterns. *Eng* **2024**, *5*, 3316–3334. [CrossRef]
20. Tomanik, E.; Christinelli, W.; Garcia, P.S.; Rajala, S.; Crepaldi, J.; Franzosi, D.; Souza, R.M.; Rovai, F.F. Effect of Graphene Nanoplatelets as Lubricant Additive on Fuel Consumption During Vehicle Emission Tests. *Eng* **2025**, *6*, 18. [CrossRef]
21. Ascencio-Hurtado, C.R.; Lázaro, R.C.A.; Estrada-López, J.J.; Jacome, A.T. Review of Si-Based Thin Films and Materials for Thermoelectric Energy Harvesting and Their Integration into Electronic Devices for Energy Management Systems. *Eng* **2023**, *4*, 1409–1431. [CrossRef]
22. Chakraborty, M.; Chatterjee, R.; Ghosh, U.U.; DasGupta, S. Electrowetting of Partially Wetting Thin Nanofluid Films. *Langmuir* **2015**, *31*, 4160–4168. [CrossRef]
23. Krishna, M.V.; Ahammad, N.A.; Chamkha, A.J. Radiative MHD flow of Casson hybrid nanofluid over an infinite exponentially accelerated vertical porous surface. *Case Stud. Therm. Eng.* **2021**, *27*, 101229. [CrossRef]
24. Azmi, W.F.W.; Mohamad, A.Q.; Jiann, L.Y.; Shafie, S. Mathematical Modelling on Pulsative MHD Blood Casson Nanofluid in Slip and Porous Capillaries for Nano-cryosurgery with Caputo-Fabrizio Approach. *Braz. J. Phys.* **2025**, *55*, 90. [CrossRef]
25. Sundar, L.S.; Deepanraj, B.; Mewada, H.K. ANFIS based effectiveness and number of transfer units predictions of MWCNT/water nanofluids flow in a double pipe U-bend heat exchanger. *Case Stud. Therm. Eng.* **2023**, *43*, 102645. [CrossRef]

26. Yan, G.; Kholoud, M.J.; Alizadeh, A.; Jasim, D.J.; Nasajpour-Esfahani, N.; Al-Shati, A.S.; Shamsborhan, M. The effect of different variables and using of the internal adiabatic wall in the construction and performance of thermosiphon heat pipes: Experimental investigation. *Case Stud. Therm. Eng.* **2023**, *50*, 103397. [CrossRef]
27. Eidan, A.A.; Alsahlani, A.; Alshukri, M.J.; Alsabery, A.I. Experimental investigation of a solar evacuated tube collector embedded with a heat pipe using different nanofluids and controlled mechanical exciting pulsations. *Int. J. Thermofluids* **2023**, *20*, 100415. [CrossRef]
28. Kaggwa, A.; Atkins, M.; Tarighaleslami, A.; Walmsley, M.; Carson, J.K. Thermal Performance of Selected Nanofluids with Surfactants. *Int. J. Thermophys.* **2023**, *44*, 160. [CrossRef]
29. Wu, H.; Zhang, L. Numerical simulation of melting of phase change material within thermal storage spiral container in existence of nanoparticles. *Case Stud. Therm. Eng.* **2023**, *52*, 103706. [CrossRef]
30. Liu, Z.; Yang, X.; Ali, H.M.; Liu, R.; Yan, J. Multi-objective optimizations and multi-criteria assessments for a nanofluid-aided geothermal PV hybrid system. *Energy Rep.* **2023**, *9*, 96–113. [CrossRef]
31. Zhu, X.; Wang, S.; Hassanvand, A.; Mousavi, S.V. Computational investigation of double non-uniform magnetic field on heat transfer of nanofluid stream along 180-degree elbow pipe. *Case Stud. Therm. Eng.* **2023**, *50*, 103416. [CrossRef]
32. Thirunavukkarasu, M.; Selvaraj, K.; Chiranjeevi, C.; Rathinavelu, V.; Maguluri, L.P.; Obaid, S.; Alharbi, S.A.; Kalam, A.M.; Yokeswaran, R. Enhancement and experimental study on thermal behaviour of heat pipe based solar absorber by using CuO nanofluid. *Therm. Sci.* **2024**, *28*, 241–247. [CrossRef]
33. Nam, H.T.; Lee, S.; Kong, M.; Lee, S. Numerical Study of Flow and Heat Transfer Characteristics for Al_2O_3 Nanofluid in a Double-Pipe Helical Coil Heat Exchanger. *Micromachines* **2023**, *14*, 2219. [CrossRef] [PubMed]
34. Smrity, A.M.A.; Yin, P. Design and performance evaluation of pulsating heat pipe using metallic nanoparticles based hybrid nanofluids. *Int. J. Heat Mass Transf.* **2024**, *218*, 124773. [CrossRef]
35. Mustafa, J.; Alqaed, S.; Sajadi, S.M.; Aybar, H.Ş. Enhancing solar panel cooling efficiency: A study on the influence of nanofluid inclusion and pin fin shape during melting and freezing of phase change materials. *Front. Energy Res.* **2024**, *12*, 1344061. [CrossRef]
36. A Abdulrahman, A. Heat pipes and nanofluids utilization for cooling photovoltaic panels: An application of hybrid machine learning and optimization models. *Int. J. Low-Carbon Technol.* **2024**, *19*, 1078–1088. [CrossRef]
37. Zhao, H. Computational modeling of nanofluid heat transfer using Fuzzy-based bee algorithm and machine learning method. *Case Stud. Therm. Eng.* **2024**, *54*, 104021. [CrossRef]
38. Najafabadi, M.K.; Hriczó, K.; Bognár, G. Entry length correlations for alumina-water nanofluid in laminar pipe flow. *Int. J. Therm. Sci.* **2024**, *197*, 108808. [CrossRef]
39. Labib, M.N.; Nine, J.; Afrianto, H.; Chung, H.; Jeong, H. International Journal of Thermal Sciences Numerical investigation on effect of base fluids and hybrid nano fluid in forced convective heat transfer. *Int. J. Therm. Sci.* **2013**, *71*, 163–171. [CrossRef]
40. Moghadassi, A.; Ghomi, E.; Parvizian, F. International Journal of Thermal Sciences A numerical study of water based Al_2O_3 and Al_2O_3—Cu hybrid nano fluid effect on forced convective heat transfer. *Int. J. Therm. Sci.* **2015**, *92*, 50–57. [CrossRef]
41. Yan, S.R.; Golzar, A.; Sharifpur, M.; Meyer, J.P.; Liu, D.H.; Afrand, M. Effect of U-shaped absorber tube on thermal-hydraulic performance and efficiency of two-fluid parabolic solar collector containing two-phase hybrid non-Newtonian nanofluids. *Int. J. Mech. Sci.* **2020**, *185*, 105832. [CrossRef]
42. Qi, J.; Ai, Q.; Zhao, P.; Yang, J.; Wang, G. Design and optimization analysis of a new double-layer tube type heat exchanger for lead-bismuth reactors. *Front. Energy Res.* **2024**, *12*, 1379747. [CrossRef]
43. Chaurasiya, P.K.; Heeraman, J.; Singh, S.K.; Verma, T.N.; Dwivedi, G.; Shukla, A.K. Exploring the combined influence of primary and secondary vortex flows on heat transfer enhancement and friction factor in a dimpled configuration twisted tape with double pipe heat exchanger using SiO_2 nano fluid. *Int. J. Thermofluids* **2024**, *22*, 100684. [CrossRef]
44. Kutakanakeri, P.A.; Narasimha, K.R.; Gopalakrishna, K.; Bhatta, L.K.G. Radial basis Neural Network Model to Prediction of Thermal Resistance and Heat Transfer Coefficient of Oscillating Heat Pipe Using Graphene and Acetone-Based Nanofluids. *Jordan J. Mech. Ind. Eng.* **2024**, *18*, 251–266. [CrossRef]
45. Islam, S.M.N.U.; Mustakim, A.; Ahamed, R.; Salehin, M.; Ehsan, M.M. Advanced Thermo-Hydraulic Assessment of Helical Pipes with Different Shapes of Jackets Using Single-Phase and Hybrid Nanofluids. *Int. J. Thermofluids* **2024**, *22*, 100628. [CrossRef]
46. Li, J.; Li, W.; Suo, R.; Guo, H.; Li, R.; Valipour, P. Influence of cross baffle on heat transfer of nanofluid flow inside circular pipe in existence of electromagnetic field: Computational study. *Case Stud. Therm. Eng.* **2024**, *59*, 104514. [CrossRef]

Disclaimer/Publisher's Note: The statements, opinions and data contained in all publications are solely those of the individual author(s) and contributor(s) and not of MDPI and/or the editor(s). MDPI and/or the editor(s) disclaim responsibility for any injury to people or property resulting from any ideas, methods, instructions or products referred to in the content.